HHS Public Access

Author manuscript

Chembiochem. Author manuscript; available in PMC 2017 June 02.

Published in final edited form as:

Chembiochem. 2016 June 02; 17(11): 999–1003. doi:10.1002/cbic.201600013.

Color-coded Super-resolution Small Molecule Imaging

Dr. Paolo Beuzer[a], **Dr. James J. La Clair**[a,b], and **Prof. Hu Cang**[a]

[a]Waitt Advanced Biophotonics Center, The Salk Institute for Biological Sciences, 10010 N Torrey Pines Rd, La Jolla, CA 92037

[b]Xenobe Research Institute, P. O. Box 3052, San Diego, CA 92163-1052

Abstract

While the development of super-resolution microscopy dates back to 1994, its applications have been primarily focused on visualizing cellular structures and targets, including proteins, DNA and sugars. We now report on a system that allows one to both monitor the localization of exogenous small molecules in live cells at low resolution and subsequently perform super resolution using stochastic optical reconstruction microscopy (STORM) on fixed cells. This represents a powerful new tool to understand the dynamics of the subcellular trafficking associated with the mode of action (MOA) of exogenous small molecules.

Graphical abstract

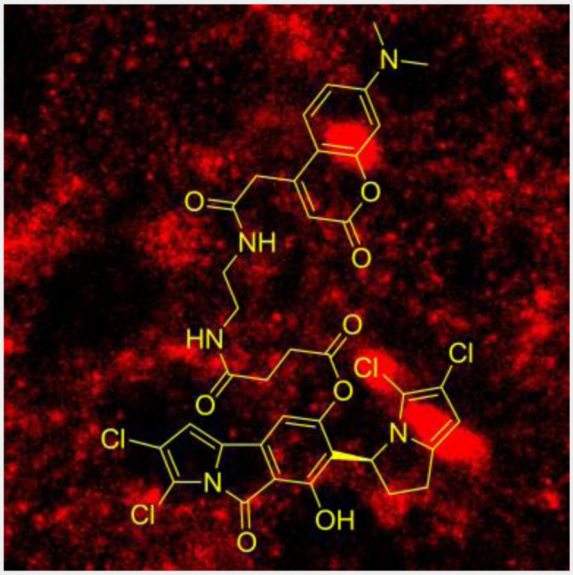

Understanding the subcellular trafficking and localization of small molecules is a fundamental aspect of chemical biology. A practical five-step procedure has now been developed that enables small molecule imaging at super-resolution. Advantageously, the method combines a color-encoded system that allows rapid uptake and tracking using a blue fluorescent immunoaffinity (IAF) tag followed by antibody based staining of fixed cells for STORM imaging.

Correspondence to: James J. La Clair; Hu Cang.

Keywords

microscopy; natural products; mode of action; drug discovery; super-resolution imaging

Small molecules, whether natural products or synthetics, offer some of the most profound means to selectively target and engage specific pathways within a cell, organism, or ecological system.[1] The diversity of roles that these molecules play is remarkable and continues to provide novel leads for the clinic, as recently exemplified by the discovery of new modes of regulating tumor cell growth[2] or advances that circumvent drug resistance in microbial infections.[3] Other roles include natural functions such as signaling communication between species,[4] or sensing key environmental clues.[5] The development of new methods to monitor the cellular and subcellular trafficking of small molecules offers a key tool to rapidly identify molecules with novel biological activity and understand their MOA.

To date, a large compendium of small molecules can be used as first line of exploration. These include an array of natively fluorescent natural products[6] and synthetic fluorescent dyes.[7] These materials, however, often have a restricted biological utility. For most bioactive materials, fluorescent probes must be prepared from their parent small molecule. This has recently been improved through the development of methods such as centralized tagging approaches, simultaneously arming and evaluating of structure activity relationships, or bioorthagonal approaches such as Click chemistry.[8]

While effective, many of these methods fail to deliver materials that can be imaged by super-resolution methods.[9] One solution to this problem arises through the development of tags optimized for super-resolution methods.[10] While an effective approach, the development of new tags is not often the central focus of a biological or drug discovery program and, hence, application of these materials often is limited to early exploratory systems.

Over the last decade, we have established a metabolically-stable tag that is small in size[8a] (Connolly's solvent excluded volume of ~210 $Å^3$), readily incorporated onto diverse natural products, and accessed by a variety of fluorescent microscopic methods. In addition, we have established an immunoaffinity fluorescent (IAF) system that uses this tag both blue fluorescent and serves as an epitope to a monoclonal antibody.[8b] Using human U2OS bone osteosarcoma cells as a model, we now demonstrate how this system can be applied to STORM imaging of small molecules.

Currently, several fluorophores suitable for STORM have been characterized, and now provide a set of five orthogonal colors.[12] In fixed cells, STORM has successfully resolved the actin cytoskeleton with a resolution of 10 nm in the lateral direction and 20 nm in the axial direction.[12] In live cells, STORM can achieve a temporal resolution of 1–2 s and spatial resolution of 30 nm and 50 nm in respective lateral and axial directions.[13] Many factors can limit STORM resolution, including: the density of the labeling, localization precision, the accuracy of the image reconstruction algorithm, the level of background noise, the thickness of a sample, and the amount of optical aberrations.[14] However, probe size is one of the most critical factors in determining the achievable spatial resolution of STORM.

Immunostaining with antibodies results in an overall 10–15 nm probe size, which can decrease the resolution by ~30 nm.[14] Smaller probes such as nanobodies or Fab fragments have been shown to partially overcome this problem.[15] Here, we demonstrate how a small dye epitope and corresponding fluorescently anti-dye antibody can be used as an optimal method for small molecule STORM.

The method begins (Step 1, Scheme 1) by treating cells with an IAF probe (see structures in Fig. 1). We applied live cell epifluorescence or confocal microscopy to monitor the cellular uptake of the IAF probe at different time points and concentrations. Once the optimal window had been identified, we proceeded to super-resolution analysis *via* STORM.

Once stained with the IAF probe, cells were fixed with 0.4% paraformaldehyde, permeabilized with 0.2% Triton, and blocked in PBS containing 0.1% Tween and 5% bovine serum albumin (Step 2, Scheme 1). The resulting sample was then treated with 80 μM Alexa 647-conjugated anti-IAF mAb XRI-TF35, a monoclonal antibody that was prepared in house as a tool for MOA studies (Step 3, Scheme 1).[8] Here, we used the blue IAF tag as the epitope for the Alexa647-conjugated mAb, therein allowing the natural product to retain its small size during cellular uptake and localization. After antibody labeling, the samples were ready for STORM analysis (Step 4, Scheme 1) and subsequent validation efforts (Step 5, Scheme 1).

To test this method, we examined three IAF-labeled natural products whose subcellular localization in mammalian cells had been examined as part of a series of drug discovery and MOA studies, namely chlorizidine A probe **1**,[17] ammosamide B probe **2**,[18] and glycyrrhetinic acid probe **3**.[8a] We began with chlorizidine A probe **1**. Our recent studies identified that chlorizidine A and associated probe **1** target two proteins within the glycolytic pathway, hENO1 and GAPDH.[17a] During the course of these studies, we found that treatment of HCT-116, a colon cancer cell line, with 10 μM **1** over 6 h resulted localization of **1** in the lysosomes, as confirmed by co-staining experiments with known lysotrackers.[16a]

Using this data, we treated U2OS cells with 50 μM probe **1** for 1 h at 37 °C in a CO_2 incubator (Step 1, Fig. 1). The cells could be inspected at any time during this period with epifluorescence or confocal microscopy using a blue fluorescent filter set, such that commonly used for imaging DAPI staining. The cells were then fixed, permeabilized, blocked (Step 2, Fig. 1) and stained with the Alexa647-conjugated anti-IAF TF35 mAb (Step 3, Fig. 1). We then imaged the resulting cells using both epifluorescence and STORM in imaging buffer (50mM Tris and10 mM NaCl pH 8 containing 40mM D-glucose, 0.5 mg/ml glucose oxidase, 40 μg/ml catalase, and 150 mM β-mercaptoethanol).

As evident in Fig. 2c, probe **1** was observed at microvesicles ranging from 200 nm to ~2 μm in size (Fig. 2c). STORM (Fig. 2d and Fig. 2f) was able to reveal details not visible by epifluorescence microscopy (Figs. 2c and Fig. 2e) or confocal microscopy.[17] In particular, small nanometer-size vesicles were observed on the perimeter of the microvesicles. This suggested that the probe initially localized at macrovescicles, but was ultimately collected over time into these nanometer-size structures within these vesicles, as observed in other

cells of the same sample (Supporting Fig. 1). Most critically, we were also able to further validate that the entire procedure did not induce any cell damage or modification in the localization of **1**. As shown by the blue epifluorescent channel in Supporting Fig. 2, the localization of **1** remained constant at all stages of the treatment and imaging process.

Using the same procedure used for chlorizidine A probe **1**, we examined the ammosamide B probe **2**. This probe was chosen as previous studies found that **2** targeted the cytoskeletal component myosin,[18a] and hence provided a new subcellular target for STORM. Both the blue fluorescence from the IAF tag (Fig. 3a) and the signal obtained after fixation, permeabilization, and staining with the Alexa647-conjugated primary antibody anti-IAF (Fig. 3b), indicated that probe **2** was diffusely localized throughout the cytoplasm. This localization was consistent with our previous observations in other tumor cell lines.[18] Higher resolution images by STORM (Fig. 3d and Fig. 3f) enabled one to identify nanometer-sized detail within this staining, however, it did not resolve fibers. This could be due to the fact that probe **2** disrupted the structure of the myosin network or that the resolution was still too low to identify the myosin fibers. Alternatively, this could arise from the lack of defined myosin fibers within the cells examined. The fact that we were able to use the blue fluorescence to monitor the IAF probe throughout the process allowed us to remove any potential concerns over alteration of the localization of probe **2** arising during fixation or permeabilization.

A final example, probe **3**, was prepared from glycyrrhetinic acid, pentacyclic triterpenoid that inhibits the enzymes, 15-hydroxyprostaglandin dehydrogenase and delta-13-prostaglandin, which metabolize the prostaglandins PGE-2 and PGF-2α.[19] Our previous studies have shown that probe **3** localizes in the endoplasmic reticulum (ER).[8a] As shown in Fig. 4, we were again able to use the blue fluorescence from **3** to identify optimally stained cells. Subcellular localization of **3** was comparable when examining epifluorescence from IAF tag (Fig. 4a) or fluorescence associated Alexa647-conjugated primary antibody anti-IAF after fixation and permeabilization (Fig. 4b). As shown, probe **3** was observed in filamentous organelles around the nucleus and was compatible with staining of the ER. Using STORM, we were able to obtain nanometric details of the structures in the ER targeted by **3**. As shown in Fig. 4d and Fig. 4f, we were able to observe large folds consistent with localization within the rough ER. Interestingly, like with probe **1**, we observed areas of increased localization density, as illustrated by arrows in Fig. 4f, within these regions suggesting that the targets of **3** were localized in specific regions of the ER.

Understanding the subcellular trafficking and localization of a small molecule is an integral part of understanding it's cellular function and MOA. Here, we described a method that allows one to image small molecule probes at super-resolution using STORM. A blue fluorescent IAF tag served as a beacon to monitor the localization of the probe throughout the experimental process and categorically reduce potential concerns due to errors during the processing and imaging steps. It also allowed us to rapidly identify conditions for staining without the need for screening on our STORM instrument. Most importantly, the uptake and localization of probes **1–3** took place in live cells, providing a more effective mimic of the natural processes of the cell. This dual-color system provides benefits that eased experimental optimization, improved quality control and provided a more reliable look at

uptake in live cells, the key of which arose from the use of a dye (IAF) and anti-dye mAb (anti-IAF) pair.

Through these studies, we were able to observe the localization of three natural product probes at high-resolution, as illustrated by the appearance of nanoscaled structures at specific organelles in Figs. 2–4. This observation indicates that the IAF tag does not alter the physiological dynamics and localization of the three analyzed small molecules. Furthermore, given its sub-nanometer size, the IAF tag represents an exciting tool for any super-resolution technique given its compatibility with immunofluorescent labeling. The development of a nanobody against the IAF tag combined with the very small size of the natural product probe offers even further potential to increase image resolution. Efforts are now underway to develop a third level of interrogation that permits further analyses as to the nature of these nanoscaled structures through counterstaining. Our focus is now exploring the use of this tool to identify pore receptors on cells as well as large macromolecular assemblies. As reported herein, this discovery offer a means to image small molecular probes in live cells, fix, and conduct super-resolution imaging with STORM to further detail this localization.

Overall, the method provides an important advancement for small molecule chemical biology and drug discovery. In particular, this method provides an excellent tool to monitor the subcellular trafficking of small molecules during their action. Here, the higher (increased) resolution available by this and related approaches[9–10] allows one to observe far greater details that simply stating that a molecule acts within a specific subcellular region of the cell. The combination of this system with conventional fluorescent antibody staining also provides a superb system to validate the binding of a small molecule to a specific target by means of co-localization studies. As described herein, super resolution provides an important next step for the chemical biological community by allowing one to observe cellular events not only within specific organelles but also within specific structural units within these organelles. We believe this approach will have an immediate application to studies that explore the MOA of small molecules.

Supplementary Material

Refer to Web version on PubMed Central for supplementary material.

Acknowledgments

This work was generously supported by funding the Salk Institute (H. C.) and the Xenobe Research Institute (J. J. L). P.B and H.C. were supported by the NIH New Innovator Award 1-DP2-EB020400, RTEF Career Development Award, and Ellison Medical Foundation New Scholar in Aging Award. We thank Prof. Willam Fenical (Scripps Institution of Oceanography) for co-development of probes **1** and **2** and Prof. Michael D. Burkart (UC San Diego) for the co-development of probe **3**.

References

1. a) Butler MS, Robertson AA, Cooper MA. Nat. Prod. Rep. 2014; 31:1612–1661. [PubMed: 25204227] b) Butler MS, Robertson AA, Cooper MA. J. Antibiot. (Tokyo). 2013; 66:571–591. [PubMed: 24002361] c) Khazir J, Riley DL, Pilcher LA, De-Maayer P, Mir BA. Nat. Prod. Commun. 2014; 9:1655–1669. [PubMed: 25532303] d) Donadio S, Maffioli S, Monciardini P, Sosio M, Jabes D. J. Antibiot. (Tokyo). 2010; 63:423–430. [PubMed: 20551985]

2. Natural products serve as a vital resource for drug leads with new modes of action. Splice modulators are one example of the recent translation of a first-in-class drug. For more information see: Hong DS, Kurzrock R, Naing A, Wheler JJ, Falchook GS, Schiffman JS, Faulkner N, Pilat MJ, O'Brien J, LoRusso P. Invest. New Drugs. 2014; 32(3):436–444. [PubMed: 24258465] Dehm SM. Clin. Cancer Res. 2013; 19:6064–6066. [PubMed: 24097858] Shi Y, Joyner AS, Shadrick W, Palacios G, Lagisetti C, Potter PM, Sambucetti LC, Stamm S, Webb TR. Pharmacol. Res. Perspect. 2015; 3:e00158. [PubMed: 26171237] Kashyap MK, Kumar D, Villa R, La Clair JJ, Benner C, Sasik R, Jones H, Ghia EM, Rassenti LZ, Kipps TJ, Burkart MD, Castro JE. Haematologica. 2015; 100:945–954. [PubMed: 25862704]
3. Natural products are also one of the leading resources for antibiotic therapy. The following manuscripts provides an excellent example of recent translational efforts: Ling LL, Schneider T, Peoples AJ, Spoering AL, Engels I, Conlon BP, Mueller A, Schäberle TF, Hughes DE, Epstein S, Jones M, Lazarides L, Steadman VA, Cohen DR, Felix CR, Fetterman KA, Millett WP, Nitti AG, Zullo AM, Chen C, Lewis K. Nature. 2015; 517:455–459. [PubMed: 25561178] Kling A, Lukat P, Almeida DV, Bauer A, Fontaine E, Sordello S, Zaburannyi N, Herrmann J, Wenzel SC, König C, Ammerman NC, Barrio NB, Borchers K, Bordon-Pallier F, Brönstrup M, Courtemanche G, Gerlitz M, Geslin M, Hammann P, Heinz DW, Hoffmann H, Klieber S, Kohlmann M, Kurz M, Lair C, Matter H, Nuermberger E, Tyagi S, Fraisse L, Grosset JH, Lagrange S, Müller R. Science. 2015; 348:1106–1112. [PubMed: 26045430]
4. An excellent example is illustrated by the complex communication in ant fungal symbiosis, see: Van Arnam EB, Ruzzini AC, Sit CS, Currie CR, Clardy J. J. Am. Chem. Soc. 2015; 137:14272–14274. [PubMed: 26535611] Sit CS, Ruzzini AC, Van Arnam EB, Ramadhar TR, Currie CR, Clardy J J. Proc. Natl. Acad. Sci. USA. 2015; 112:13150–13154. [PubMed: 26438860]
5. The induction of dauer in *Caenorhabditis elegans* by daumone and related ascerolides is also an excellent example of environmental cues, see: Bose N, Meyer JM, Yim JJ, Mayer MG, Markov GV, Ogawa A, Schroeder FC, Sommer RJ. Curr. Biol. 2014; 24:1536–1541. [PubMed: 24980503] Choe A, Chuman T, von Reuss SH, Dossey AT, Yim JJ, Ajredini R, Kolawa AA, Kaplan F, Alborn AT, Teal PE, Schroeder FC, Sternberg PW, Edison AS. Proc. Natl. Acad. Sci. USA. 2012; 109:20949–20954. [PubMed: 23213209] Baiga TJ, Guo H, Xing Y, O'Doherty GA, Dillin A, Austin MB, Noel JP, La Clair JJ. ACS Chem. Biol. 2008; 3:294–304. [PubMed: 18376812]
6. An excellent example is the commercial development of epicocconone Peixoto PA, Boulangé A, Ball M, Naudin B, Alle T, Cosette P, Karuso P, Franck X. J. Am. Chem. Soc. 2014; 136:15248–15256. [PubMed: 25271695] Choi HY, Veal DA, Karuso P. J. Fluoresc. 2006; 16:475–482. [PubMed: 16328703] García-Plazaola JI, Fernández-Marín B, Duke SO, Hernández A, López-Arbeloa F, Becerril JM. Plant Sci. 2015; 236:136–145. [PubMed: 26025527]
7. An excellent example of modern methods include the combinatorial development of fluorescent dyes, see: Yun SW, Kang NY, Park SJ, Ha HH, Kim YK, Lee JS, Chang YT. Acc. Chem. Res. 2014; 47:1277–1286. [PubMed: 24552450] Vendrell M, Zhai Z, Er JC, Chang YT. Chem. Rev. 2012; 112:4391–4420. [PubMed: 22616565]
8. a) Alexander MD, Burkart MD, Leonard MS, Portonovo P, Liang B, Ding X, Joullié MM, Gulledge BM, Aggen JB, Chamberlin AR, Sandler J, Fenical W, Cui J, Gharpure SJ, Polosukhin A, Zhang HR, Evans PA, Richardson AD, Harper MK, Ireland CM, Vong BG, Brady TP, Theodorakis EA, La Clair JJ. Chembiochem. 2006; 7:409–416. [PubMed: 16432909] b) Yu WL, Guizzunti G, Foley TL, Burkart MD, La Clair JJ. J Nat Prod. 2010; 73:1659–1666. [PubMed: 20836515] c) Heisig F, Gollos S, Freudenthal SJ, El-Tayeb A, Iqbal J, Müller CE. J. Fluoresc. 2014; 24:213–230. [PubMed: 24052460] d) Flores-Rizo JO, Esnal I, Osorio-Martínez CA, Gómez-Durán CF, Bañuelos J, López Arbeloa I, Pannell KH, Metta-Magaña AJ, Peña-Cabrera E E. J. Org. Chem. 2013; 78:5867–5877. [PubMed: 23721096] e) Haldar S, Kumar S, Kolet SP, Patil HS, Kumar D, Kundu GC, Thulasiram HV. J. Org. Chem. 2013; 78:10192–10202. [PubMed: 24079457] f) Robles O, Romo D. Nat. Prod. Rep. 2014; 31:318–334. [PubMed: 24468713] g) Li J, Cisar JS, Zhou CY, Vera B, Williams H, Rodríguez AD, Cravatt BF, Romo D. Nat. Chem. 2013; 5:510–517. [PubMed: 23695633] h) Chamni S, He QL, Dang Y, Bhat S, Liu JO, Romo D. ACS Chem. Biol. 2011; 6:1175–1181. [PubMed: 21894934] i) Ma N, Wang Y, Zhao BX, Ye WC, Jiang S. Drug. Des. Devel. Ther. 2015; 9:1585–1599.j) Mamidyala SK, Finn MG. Chem. Soc Rev. 2010; 39:1252–1261. [PubMed: 20309485]

9. a) Kaufmann R, Hagen C, Grünewald K. Curr. Opin Chem. Biol. 2014; 20:86–91. [PubMed: 24951858] b) Stennett EM, Ciuba MA, Levitus M. Chem. Soc. Rev. 2014; 43:1057–1075. [PubMed: 24141280]
10. a) Grimm JB, English BP, Chen J, Slaughter JP, Zhang Z, Revyakin A, Patel R, Macklin JJ, Normanno D, Singer RH, Lionnet T, Lavis LD. Nat. Methods. 2015; 12:244–520. [PubMed: 25599551] b) Viswanathan S, Williams MW, Bloss EB, Stasevich TJ, Speer CM, Nern A, Pfeiffer BD, Hooks BM, Li WP, English BP, Tian T, Henry GL, Macklin JJ, Patel R, Gerfen CR, Zhuang X, Wang Y, Rubin GM, Looger LL. Nat. Methods. 2015; 12:568–576. [PubMed: 25915120] c) Lee MK, Rai P, Williams J, Twieg RJ, Moerner WE. J. Am. Chem. Soc. 2014; 136:14003–14006. [PubMed: 25222297] d) Zheng Q, Juette MF, Jockusch S, Wasserman WR, Zhou Z, Altman RB, Blanchard SC. Chem. Soc. Rev. 2014; 3:1044–1056.e) van de Linde S, Aufmkolk S, Franke C, Holm T, Klein T, Löschberger A, Proppert S, Wolter S, Sauer M. Chem. Biol. 2013; 20:8–18. [PubMed: 23352135] f) Lin J, Wester WJ, Graus MS, Lidke KA, Neumann AK. Mol. Biol. Cell. 2016 Jan 20. mbc.E15-06-0355. g) Jiang H, English BP, Hazan RB, Wu P, Ovryn B. Angew. Chem. Int. Ed. Engl. 2015; 54:1765–1769. [PubMed: 25515330] h) Chen J, Gao J, Wu J, Zhang M, Cai M, Xu H, Jiang J, Tian Z, Wang H. Nanoscale. 2015; 7:3373–3380. [PubMed: 25630278]
11. a) Almada P, Culley S, Henriques R. Methods. 2015; 88:109–121. [PubMed: 26079924] b) Yamanaka M, Smith NI, Fujita K. Microscopy (Oxf). 2014; 63:177–192. [PubMed: 24671128] c) Oddone A, Vilanova IV, Tam J, Lakadamyali M. Microsc. Res. Tech. 2014; 77:502–509. [PubMed: 24616244] d) Betzig E, Patterson GH, Sougrat R, Lindwasser OW, Olenych S, Bonifacino JS, Davidson MW, Lippincott-Schwartz J, Hess HF. Science. 2006; 313:1642–1645. [PubMed: 16902090] e) Bates M, Huang B, Dempsey GT, Zhuang X X. Science. 2007; 317:1749–1753. [PubMed: 17702910] f) Patterson G, Davidson M, Manley S, Lippincott-Schwartz J. Annu. Rev. Phys. Chem. 2010; 61:345–367. [PubMed: 20055680]
12. Tam J, Cordier GA, Borbely JS, Sandoval Álvarez A, Lakadamyali M. PLoS One. 2014; 9:e101772. [PubMed: 25000286]
13. Xu K, Babcock HP, Zhuang X. Nat. Methods. 2012; 9:185–188. [PubMed: 22231642]
14. a) Jones SA, Shim SH, He J, Zhuang X X. Nat. Methods. 2011; 8:499–508. [PubMed: 21552254] b) Hu YS, Nan X, Sengupta P, Lippincott-Schwartz J, Cang H. Nat. Meth. 2013; 10:96–97.c) Shroff H, Galbraith CG, Galbraith JA, Betzig E. Nat. Meth. 2008; 5:96–97.d) Gebhardt JCM, Suter DM, Roy R, Zhao ZW, Chapman AR, Basu S, Maniatiss T, Xie XS. Nat. Meth. 2013; 10:421–426.e) Hu YS, Zhu Q, Elkins K, Tse K, Li Y, Fitzpatrick JAJ, Verma IM, Cang H. Opt. Nanoscopy. 2013:2–7.f) Huang B, Jones SA, Brandenburg B, Zhuang X. Nat. Meth. 2008; 5:1047–1052.g) Small A, Stahlheber S S. Nat. Meth. 2014; 11:267–279.
15. a) Veatch SL, Machta BB, Shelby SA, Chiang EN, Holowka DA, Baird BA. PLoS One. 2012; 7:e31457. [PubMed: 22384026] b) Lakadamyali M, Babcock H, Bates M, Zhuang X, Lichtman J. PLoS One. 2012; 7:e30826. [PubMed: 22292051] c) Wolter S, Schüttpelz M, Tscherepanow M, van de Linde S, Heilemann M, Sauer M. J. Microsc. 2010; 237:12–22. [PubMed: 20055915] d) Dedecker P, Duwé S, Neely RK, Zhang J. J. Biomed. Opt. 2012; 17:126008. [PubMed: 23208219] e) Dedecker P, Mo GC, Dertinger T, Zhang J. Proc. Natl. Acad. Sci. USA. 2012; 109:10909–10914. [PubMed: 22711840] f) Tehrani KF, Xu J, Zhang Y, Shen P, Kner P. Opt. Express. 2015; 23:13677–13692. [PubMed: 26074617] g) Quirin S, Pavani SR, Piestun R. Proc. Natl. Acad. Sci. USA. 2012; 109:675–679. [PubMed: 22210112]
16. a) Mikhaylova M, Cloin BM, Finan K, van den Berg R, Teeuw J, Kijanka MM, Sokolowski M, Katrukha EA, Maidorn M, Opazo F, Moutel S, Vantard M, Perez F, van Bergen en Henegouwen PM, Hoogenraad CC, Ewers H, Kapitein LC. Nat. Commun. 2015; 6:7933. [PubMed: 26260773] b) Pleiner T, Bates M, Trakhanov S, Lee CT, Schliep JE, Chug H, Böhning M, Stark H, Urlaub H, Görlich D. Elife. 2015; 4:e11349. [PubMed: 26633879] c) Platonova E, Winterflood CM, Junemann A, Albrecht D, Faix J, Ewers H. Methods. 2015; 88:89–97. [PubMed: 26123185] d) Bates M, Jones SA, Zhuang X. Cold Spring Harb. Protoc. 2013; 2013:540–541. [PubMed: 23734027]
17. a) Álvarez-Micó X, Rocha DD, Guimarães LA, Ambrose A, Chapman E, Costa-Lotufo LV, La Clair JJ, Fenical W. Chembiochem. 2015; 16:2002–2006. [PubMed: 26267855] b) Álvarez-Micó X, Jensen PR, Fenical W, Hughes CC. Org. Lett. 2013; 15:988–991. [PubMed: 23405849]
18. a) Hughes CC, MacMillan JB, Gaudêncio SP, Fenical W, La Clair JJ. Angew. Chem. Int. Ed. Engl. 2009; 48:728–732. *Angew. Chem.* **2009**, *121*, 742–746. [PubMed: 19097126] b) Hughes CC,

MacMillan JB, Gaudêncio SP, Jensen PR, Fenical W. Angew. Chem. Int. Ed. Engl. 2009; 48:725–727. *Angew. Chem.* **2009**, *121*, 739–741. [PubMed: 19090514]

19. a) Patel FA, Sun K, Challis JR. J. Clin. Endocrinol. Metab. 1999; 84:395. [PubMed: 10022390] b) Peskar BM, Teelucksingh S, Benediktsson R, Lindsay RS, Burt D, Seckl JR, Edwards CN, Nan CL, Kelly R. Lancet. 1991; 337:1549. [PubMed: 1675399]

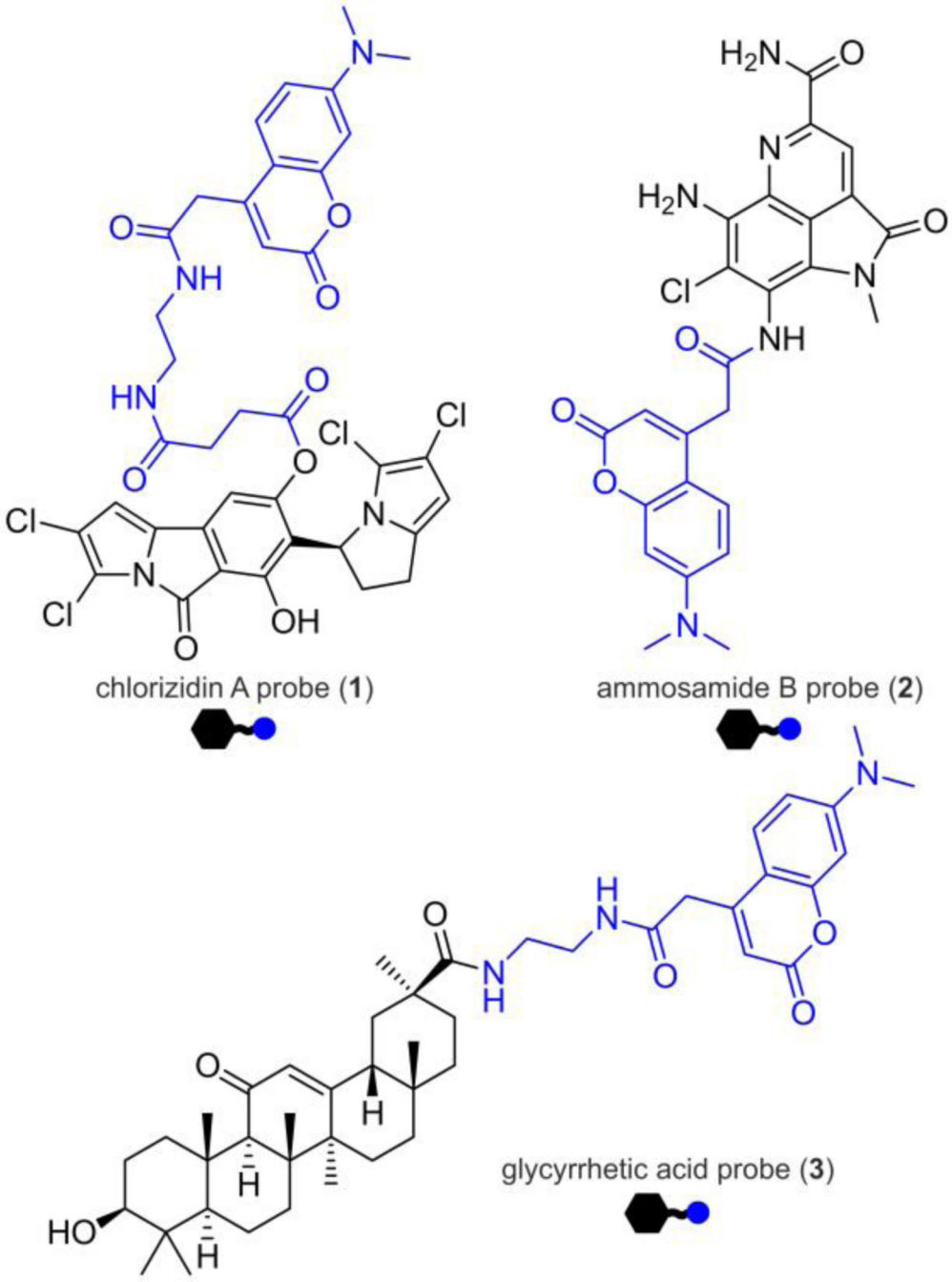

Figure 1.
Structures of IAF probes **1**–**3** including the core pharmacological unit (black) and associated IAF tag (blue).

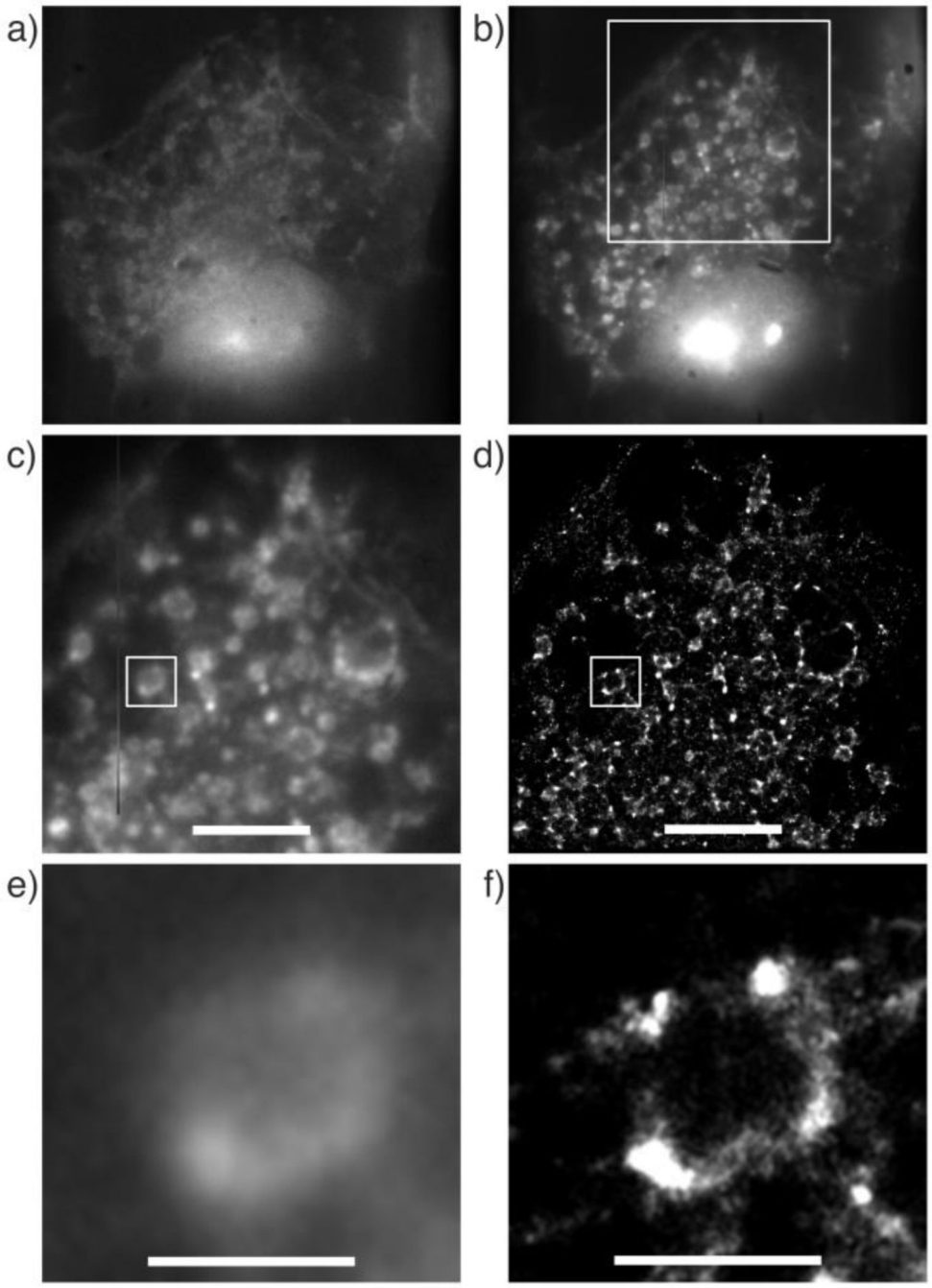

Figure 2.

Color-coded STORM imaging of clorizidine A probe (**1**). U2OS cells were treated with 50 μM blue-fluorescent **1** for 1 h in DMEM buffer at 37 °C in an atmosphere of 5% CO_2. **a)** Blue epifluorescence image from **1** upon excitation at 385–400 nm with emission collected at 450–465 nm. **b)** Epifluorescence image depicting the cells after immunolabeling for 1 h at 23 °C with 80 μM Alexa647-conjugated anti-IAF TF35 mAb with excitation at 590–650 nm and fluorescence collected 663–738 nm. **c)** An expansion of the boxed region of the cell in b). **d)** Corresponding STORM image to c). **e)** An expansion the boxed region of the cell in

c). **f)** Corresponding STORM image to e). Scale bars are given by 5 μm in c) and d) and 1 μm in e) and f).

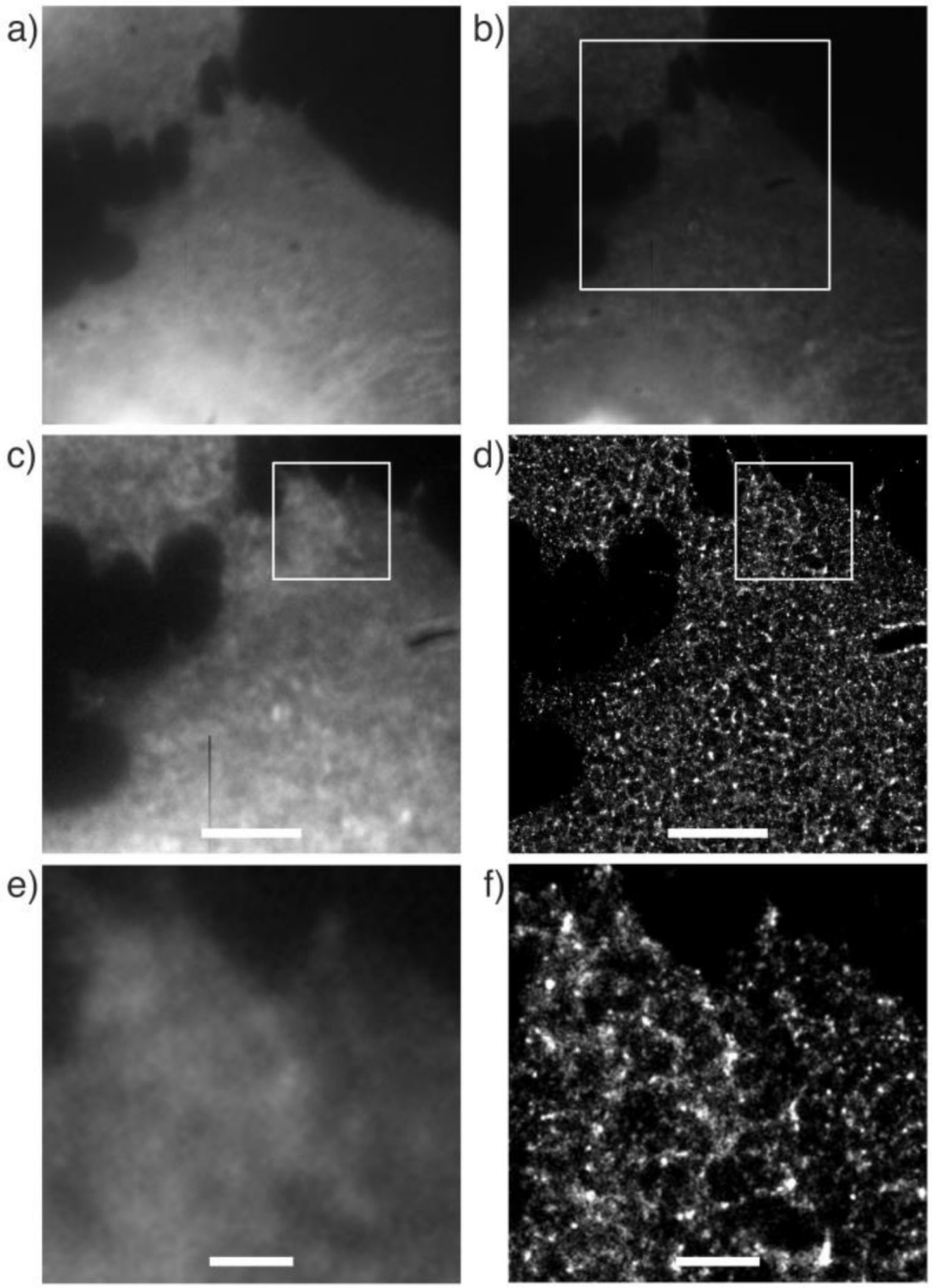

Figure 3.

Color-coded STORM imaging of ammosamide B probe (**2**). U2OS cells were treated with 50 μM blue-fluorescent **2** for 1 h in DMEM buffer at 37 °C in an atmosphere of 5% CO_2. **a)** Blue epifluorescence image from **2** upon excitation at 385–400 nm with emission collected at 450–465 nm. **b)** Epifluorescence image depicting the cells after immunolabeling for 1 h at 23 °C with 80 μM Alexa647-conjugated anti-IAF TF35 mAb with excitation at 590–650 nm and fluorescence collected 663–738 nm. **c)** An expansion of the boxed region of the cell in b). **d)** Corresponding STORM image to c). **e)** An expansion the boxed region of the cell in

c). **f)** Corresponding STORM image to e). Scale bars are given by 5 μm in c) and d) and 1 μm in e) and f).

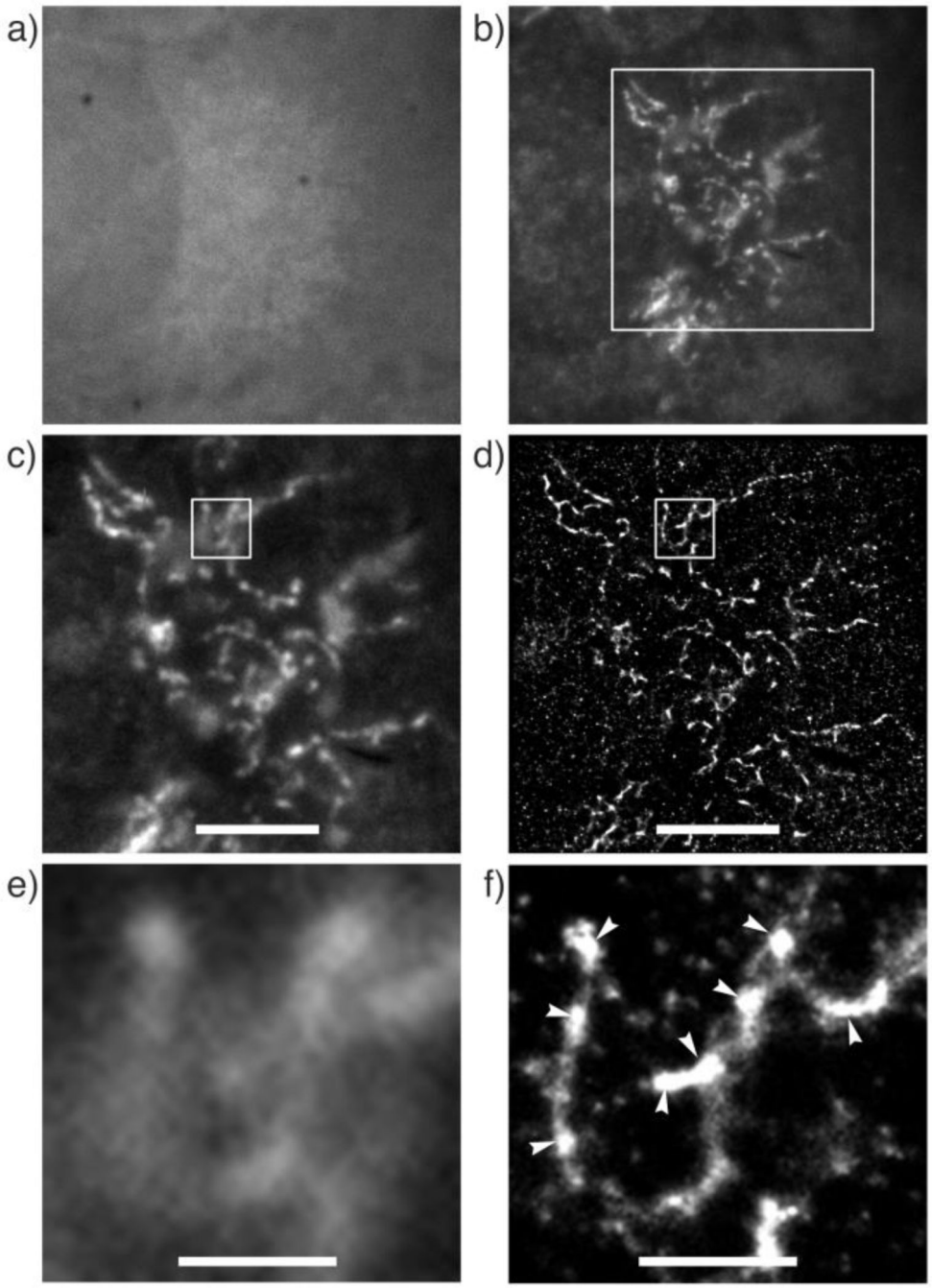

Figure 4.

Color-coded STORM imaging of glycyrrhetinic acid probe (**3**). U2OS cells were treated with 50 μM blue-fluorescent **1** for 1 h in DMEM buffer at 37 °C in an atmosphere of 5% CO_2. **a)** Blue epifluorescence image from **1** upon excitation at 385–400 nm with emission collected at 450–465 nm. **b)** Epifluorescence image depicting the cells after immunolabeling for 1 h at 23 °C with 80 μM Alexa647-conjugated anti-IAF TF35 mAb with excitation at 590–650 nm and fluorescence collected 663–738 nm. **c)** An expansion of the boxed region of the cell in b). **d)** Corresponding STORM image to c). **e)** An expansion the boxed region of

the cell in c). **f)** Corresponding STORM image to e). Scale bars are given by 5 μm in c) and d) and 1 μm in e) and f).

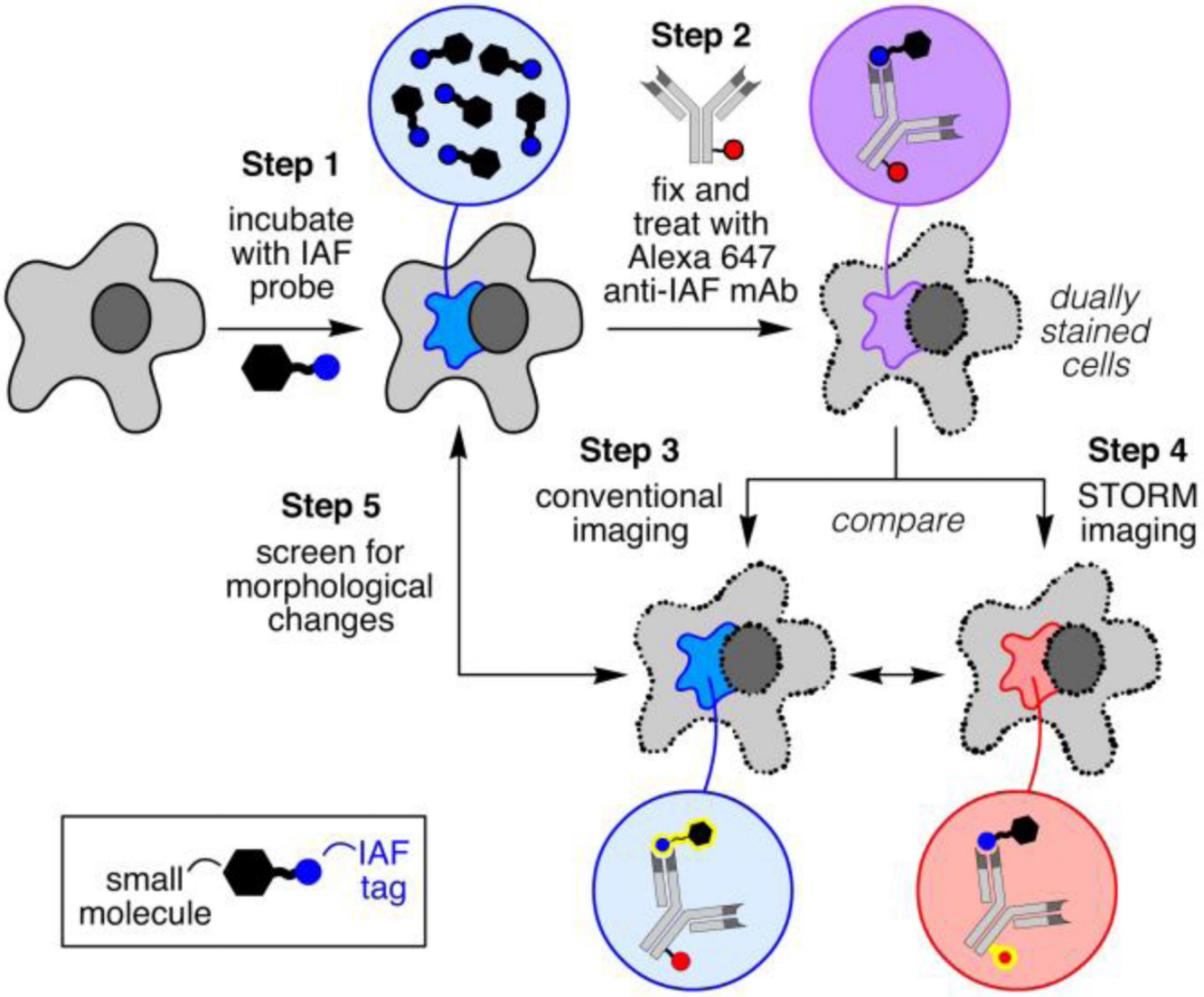

Scheme 1.

Color-coded super-resolution microscopy. A five-step procedure for parallel inspection of fluorescent small molecule localization that uses a combination of an IAF probe and corresponding Alexa 647-conjugated anti-IAF mAb with epifluorescence or confocal microscopy and STORM imaging. (insert, upper left) An IAF probe is comprised of a small molecule (grey) covalently-labeled with an IAF tag (blue sphere). Circular expansions depict localization of the IAF-probe and subsequent staining with an Alexa 647-conjugated (red sphere) anti-IAF mAb. These expansions are colored according to the use of conventional (blue) or STORM (red) imaging with the fluorescent unit explored highlighted in yellow.